

DOI: 10.1002/icc.26210

## FULLPAPER



# Acylation and deacylation mechanism and kinetics of penicillin G reaction with Streptomyces R61 DD-peptidase

Qianyi Cheng 0

Nathan J. DeYonker 💿

Department of Chemistry, University of Memphis, Memphis, Tennessee

#### Correspondence

Qianyi Cheng and Nathan J. DeYonker, Department of Chemistry, University of Memphis, Memphis, TN

Email: qcheng1@memphis.edu (Q. C.) and Email: ndyonker@memphis.edu (N. J. D.)

## **Funding information** University of Memphis Department of Chemistry; University of Memphis, College of Arts and Sciences; the National Science

Foundation, Grant/Award Number: BIO-1846408

#### INTRODUCTION 1

For most bacteria, the cell wall is essential to survival, providing the bacteria with not only structural support but also protection. The bacterial cell wall is a mesh-like layer outside the plasma membrane, which is formed with peptidoglycan—a polymer consisting of sugars and amino acids. The bacterial enzyme D-

alanyl-p-alanine transpeptidase ("DD-peptidase" in short) is indispensable as it catalyzes the cross-linking between amino acids (peptide side chains) in different linear amino sugar chains of the peptidoglycan, forming the strong and rigid 3-dimensional structure of the cell wall.[1]

The active site of DD-peptidase enzymes contains a highly conserved serine  $residue^{\text{[2]}}$  and the serine  $\gamma\text{-OH}$  group cleaves the D-alanyl-D-alanine bond of a peptide, covalently bonding to the produced acyl-fragment (carbonyl donor) and forming an acyl-enzyme complex. Then the acylenzyme complex breaks down, resulting in the formation of a new peptide bond between the carbonyl of the D-alanyl moiety and the amino group of another peptide unit. The essential biological role of DD-peptidase has made it an excellent drug target for killing bacteria. β-lactam antibiotics (examples shown in Figure 1) such as cephalosporins (Figure 1b) and

#### **Abstract**

Two quantum mechanical (QM)-cluster models are built for studying the acylation and deacylation mechanism and kinetics of Streptomyces R61 DD-peptidase with the penicillin G at atomic level detail. DD-peptidases are bacterial enzymes involved in the cross-linking of peptidoglycan to form the cell wall, necessary for bacterial survival. The cross-linking can be inhibited by antibiotic beta-lactam derivatives through acylation, preventing the acylenzyme complex from undergoing further deacylation. The deacylation step was predicted to be rate-limiting. Transition state and intermediate structures are found using density functional theory in this study, and thermodynamic and kinetic properties of the proposed mechanism are evaluated. The acylenzyme complex is found lying in a deep thermodynamic sink, and deacylation is indeed the severely rate-limiting step, leading to suicide inhibition of the peptidoglycan cross-linking. The usage of QM-cluster models is a promising technique to understand, improve, and design antibiotics to disrupt function of the Streptomyces R61 DD-peptidase.

KEYWORDS

DD-peptidase, DFT, QM-cluster models, quantum mechanics

penicillin derivatives (Figure 1c) are known to be important clinical defenses against bacterial infections. [5,6] The β-lactam ring in the antibiotics has a similar Dalanyl-D-alanine motif to the peptidoglycan, which kills bacteria by inactivating the enzyme DD-peptidases and inhibiting the crosslinking step in the cell wall biosynthesis.[7-9]

The investigation of DD-peptidase reaction mechanisms and kinetics was pioneered by Frère and coworkers[10-18] and is still an active area of research for academia[10-12] and for pharmaceutical companies as they try to design safe and efficient drugs and antibiotics. [13] Two prominent antibiotics primarily serve as DD-peptidase inhibitors, which are cephalosporins (such as cephalothin in Figure 1d) and penicillins (such as benzylpenicillin, also called penicillin G in Figure 1e, or 6-(Glycyl- $_{L}$ - $\alpha$ -aminopimelyl)aminopenicillananic acid in

J Comput Chem. 2020;41:1685-1697. wileyonlinelibrary.com/journal/jcc © 2020 Wiley Periodicals, Inc. 1685

(a) 2-Azetidinone, the simplest  $\beta$ -lactam

(b) Cephalosporin

(c) Penicillin

(f) Perfect Penicillin

Figure 1f, which is the most effective known  $\beta$ -lactam inhibitor of DD-peptidase and dubbed a "perfect penicillin").[14,15]

Interestingly, it has been found that cephalosporins are poorer inhibitors than penicillins in Streptomyces sp. strain R61 DD-peptidase enzyme. [14] Despite kinetic experiments showing even slower rate constants for peptidoglycan deacylation, the observed acyl-enzyme binding rate constants are nearly 10 times slower for cephalosporin C, [16] and even slower for second- and third-generation

cephalosporins.[17]

Multiple experimental studies have examined the proposed mechanism of penicillin G with Streptomyces sp. strain R61 DD-peptidase. [7,8,18,19] It is proposed that the deacylation step may be initiated by water and a general base via nucleophilic attack on the carbonyl carbon of the acyl-group. The slow reaction is caused by steric hindrance of the heterocyclic ring and is proposed to be rate-limiting. [3,4,20] A rate-limiting deacylation step for inhibition also explains successful efforts to crystallographically "trap" the covalently bound acyl-complex of penicillin G in Streptomyces sp. strain R61 DD-peptidase. [14] The bound acyl-enzyme

FIGURE 1 Structure of (a) the simplest  $\beta$ -lactam, (b) Cephalosporin, (c) Penicillin, (d) Cephalothin,

(e) Benzylpenicillin (penicillin G) and (f) 6- (Glycyl- $_{\text{L}}$ - $\alpha$ -aminopimelyl)aminopenicillananic acid, which has been suggested to be a "Perfect Penicillin" in Kuzin et al. [3] and Powers et al. [4]

complex has been found to lie in a thermodynamic sink, with an extremely high effective activation energy needed for deactivation, which slows biological transpeptidase function. [19]

Various mutational, enzyme kinetic, crystallographic, and computational studies on DD-peptidases and class A and class C Blactamases (produced by bacteria and resistant to β-lactam antibiotics, ABL and CBL in short) have devoted extensive discussion to proton transfer throughout the mechanism.[17,21-51] A proton must be removed from the active site serine hydroxyl group and another proton must be added to the amine leaving group; similar proton transfer must be facilitated during the deacylation mechanism. Although structural information is available on these enzymes and enzyme-ligand complexes, illustration of the reaction mechanism and activity is still unclear due to multiple possible protonation states for some important residues.<sup>[45]</sup> Uncertainty in the catalytic protonation state is also related to which residue acts as the general base/acid in the acylation and deacylation. Also, the importance of residues His298,[52] Asn161,[17]

Tyr159,<sup>[48]</sup> Thr299,<sup>[49]</sup> and Tyr280<sup>[53]</sup> has been identified by various mutation experiments, and Asn161 is the most important in the transfer mechanism among these residues.

Computational studies on the acylation and deacylation reactions of ABL and CBL have provided additional quantitative validation of the thermodynamics and kinetics. A high energy tetrahedral acylation intermediate (acyl-enzyme complex) was proposed. [51,54,55] Molecular dynamics (MD) simulation studies found that in the aztreonam/CBL noncovalent complex, the K+Y- reactant is less stable than K<sup>0</sup>Y<sup>0</sup>, [56] but both protonation states have been found to be accessible at ambient conditions in a quantum mechanical/molecular mechanical (QM/MM) study of the cephalothin-CBL noncovalent complex. [29] For deacylation, a QM/MM study of the cephalothin-CBL acyl-enzyme complex showed that K+Y- is lower in energy compared to K<sup>0</sup>Y<sup>0</sup>, [57,58] and it was also found that the hydrogen bond between Lys67 and Tyr150 is important for deacylation. The activation free-energy of cephalothin deacylation was predicted to be 12 [59] and 14 [57] kcal mol<sup>-1</sup> by QM/MM studies for the drug-resistant enzymes. A quantum

mechanical (QM)-cluster model study on CBL using Density Functional Theory (B3LYP/6-31G\*\*) with a very small 72-atom model found an activation energy for the deacylation process of

30 kcal mol $^{-1}$ .[58] In that QM-cluster model study, a deacylation tetrahedral intermediate was predicted to be only 3.5 kcal mol $^{-1}$  lower in energy than the rate-limiting transition state[58] with a water molecule in close proximity to Tyr150.[58,59] Frequent proton transfer between Lys67 and Tyr150 was observed in these previous computational studies, with Tyr150 more likely in the deprotonated form.[57,59]

In contrast, QM/MM investigation of the deacylation (hydrolysis) of cephalothin-R61 PBP (a non-drug resistant DD-peptidase) indicated two different pathways, where Tyr150 acts as the general base, as well as a second proposed mechanism involving concerted proton transfer between Tyr150/Lys67. The activation free energy of deacylation was predicted to be 49 and 40 kcal mol<sup>-1</sup>, respectively.<sup>[57]</sup>

In this work we will employ QM-cluster modeling to study the complete acylation and deacylation reaction mechanism of penicillin G with a penicillin binding protein (PBP, PDB ID: 1PWC<sup>[14]</sup>). As in all QM and QM/MM enzyme mechanism studies, defining the mechanistically relevant active site and locating catalytic residues in the enzyme is crucial.<sup>[60]</sup>

In the active site of proteins, the idea of residue interaction networks (RINs) has been proposed, [61,62] which provide additional quantitative insights into the structural and functional role of residues and inter-residue interactions. RINs have been applied in studying identification of key residues for protein folding [63,64] and functionally distinct protein states. [65,66] In our lab, RINs have been used for guided QM-cluster model creation with a systematic and reproducible increase in model size. This approach has been successfully applied in studying phosphoryl transfer mechanisms within the Phospholipase D[67] and Tyrosyl-DNA phosphodiesterase I enzymes, [68] as well as a recent study of biphenyl dihedral angle rotation in the bioengineered Threonyl-tRNA synthetase. [69] In this work, we have applied RINs to identify important residues in the acylation and deacylation reaction of penicillin G in an enzyme model of the 1PWC X-ray crystal structure, to give atomic-level, quantitative answers to the following questions:

- 1 What residue acts as the general base in this enzyme in acylation and deacylation?
- 2 What role do water molecules play in acylation and deacylation?
- 3 How do we reconcile the sometimes-large differences in acylation/ deacylation kinetics between experimental and computational studies?
- 4 How can we better utilize RINs in constructing QM enzyme models?

## 2 | METHODS

The X-ray crystal structure of the penicilloyl acyl enzyme complex (Streptomyces R61 DD-peptidase bound with penicillin G, PDB ID: 1PWC) was used to construct the models for quantum mechanical computations.

H atoms were added using the reduce program, [70] then the protonated PDB file was further treated by probe<sup>[71]</sup> to generate atom contact information. A residue interaction network (RIN) was constructed based on the active site including the penicillin G ligand (PNM, and Figure 2 shows the atom numbering in PNM) and the residue Ser62, which PNM is directly bonded to. From analysis of RIN results, 17 residues from chain A directly interact with Ser62 and/or PNM400 via either hydrogen bonds, bad atomic overlaps (steric clashes), or non-overlapped van der Waals contacts (close contacts)[71]: Val60, Gly61, Ser62, Val63, Thr64, Lys65, Phe120, Tyr159, Asn161, Trp233, Ala237, Gly238, Arg285, His298, Thr299, Gly300, and Thr301, and four explicit waters (wat1014, wat1025, wat1108, and wat1465). Also based on the generated RIN, either main chain, side chain, or entire residues were trimmed and treated to fulfill atom valency in the model. It should be noted that Hargis and Woodcock found that doubly protonated His298 ( $N_{\epsilon}$  and  $N_{\delta}$ ) might be required for facile acylation.<sup>[31]</sup> Therefore, two different models were generated by our in-house program package Residue Interaction Networkbased ResidUe Selector (RINRUS) and were used to explore mechanistic differences arising from the protonation state of His298. The first model contains 277 atoms (His298 N<sub>€</sub> protonated as pH = 6.8 for the experimental condition) with 17  $C_{\alpha}$  atoms frozen and 5 C<sub>B</sub> atoms frozen (in Phe120, Tyr159, Asn161, Trp233, and Arg285). The second model only differs by containing double protonation of the His298 residue (278 atoms with the same 22 frozen atoms specified above).

All quantum mechanical cluster model computations were performed using the Gaussian16 program. [72] Density functional theory (DFT) with the hybrid B3LYP exchange-correlation functional [73,74] was employed with the  $6-31G(d^0)$  basis set for N, O, and S

atoms<sup>[75–77]</sup> and the 6-31G basis sets for C and H atoms.<sup>[78]</sup> Models

$$C_{10}$$
 $C_{10}$ 
 $C_{10}$ 
 $C_{2}$ 
 $C_{3}$ 
 $C_{11}$ 
 $C_{10}$ 
 $C_{2}$ 
 $C_{3}$ 
 $C_{11}$ 
 $C_{10}$ 
 $C_{2}$ 
 $C_{3}$ 
 $C_{11}$ 
 $C_{11}$ 
 $C_{12}$ 
 $C_{12}$ 
 $C_{15}$ 
 $C_{15}$ 
 $C_{16}$ 
 $C_{16}$ 
 $C_{10}$ 
 $C_{10}$ 

FIGURE 2 Atom numbering in Penicillin G in complex with Serine 62 in the penicilloyl acyl-enzyme complex

in implicit solvent incorporated the Grimme D3 (Becke-Johnson) dispersion correction (GD3BJ)<sup>[79,80]</sup> and a conductor-like polarizable continuum model (CPCM)<sup>[81,82]</sup> with cavity built up using the universal force field (UFF) atomic radii where hydrogens have explicit individual spheres, a non-default electrostatic scaling factor of 1.2, and a dielectric constant of  $\varepsilon$  = 4. This dielectric constant value has been previously determined as appropriate for simulating the less-polarized environment within an enzyme active site.<sup>[83,84]</sup> Unscaled harmonic vibrational frequency calculations were used to identify all stationary points as either minima (no imaginary frequency) or transition states (only one imaginary frequency). Zero-point energies (ZPE) and thermal enthalpy/free energy corrections were computed at 1 atm and 298.15 K, which are reported in Supporting Information, Tables S1 and S2.

It should be noted that previous QM-cluster model studies in our group report relative free energies,  $^{[68,69]}$  whereas in this study, we use non-vibrationally corrected relative energies at 0 K ( $\Delta E_{\rm e}$ ). Some elementary steps in the proposed mechanisms below are effectively barrierless when comparing relative electronic energies. However, when imaginary vibrational modes are of large magnitude, their removal from zero-point energy and partition functional calculations results in a situation where TSs have lower relative free energies than either the corresponding reactant or product. This does not suggest a catastrophic failure of our QM-cluster model or the methodology employed. Rather, these stationary points are not minima or maxima on the free energy surface but are still treated as such to adhere to the Principle of Microscopic Reversibility on the electronic energy surface.  $^{[85]}$  More discussion on this nuance is provided in the Supporting Information.

## 3 | RESULTS AND DISCUSSION

Energy diagrams of the computed acylation and deacylation reaction of Streptomyces R61 DD-peptidase with penicillin G via the 277-atom model (label starts with A) and the 278-atom model (label starts with B) in solution phase are shown in Figures 3 and 4. Thermochemical data for all minima/maxima of the penicillin G reaction with Streptomyces R61 DD-peptidase is listed in Supporting Information.

A total of 17 stationary points were found in the solution phase for the 277-atom model pathway, including 9 minima and 8 transition states (TS); while 15 stationary points (8 minima and 7 TS) were found for the 278-atom model pathway (Figures 5 and 6). For comparison of relative energies, the respective energies of A-1 and B-1 are used as the reference ( $\Delta E = 0.0$  kcal mol<sup>-1</sup>). Structures A-1 to A-7 in Schemes 1–3 correspond to the formation of the acyl-complex (acylation); A-7 to A-9 in Schemes 4 and 5 are for dissociation of the acylcomplex (deacylation). Structures B-1 to B-6 correspond to the formation of the acyl-complex (acylation); B-6 to B-8 are

for deacylation of the acyl-complex (deacylation). The initial models were constructed based on the penicilloyl acyl-enzyme complex (the A-7, A-8 and B-6, B-7 structures), which closely resemble the X-ray crystal structure after geometry optimization (Figure 7).

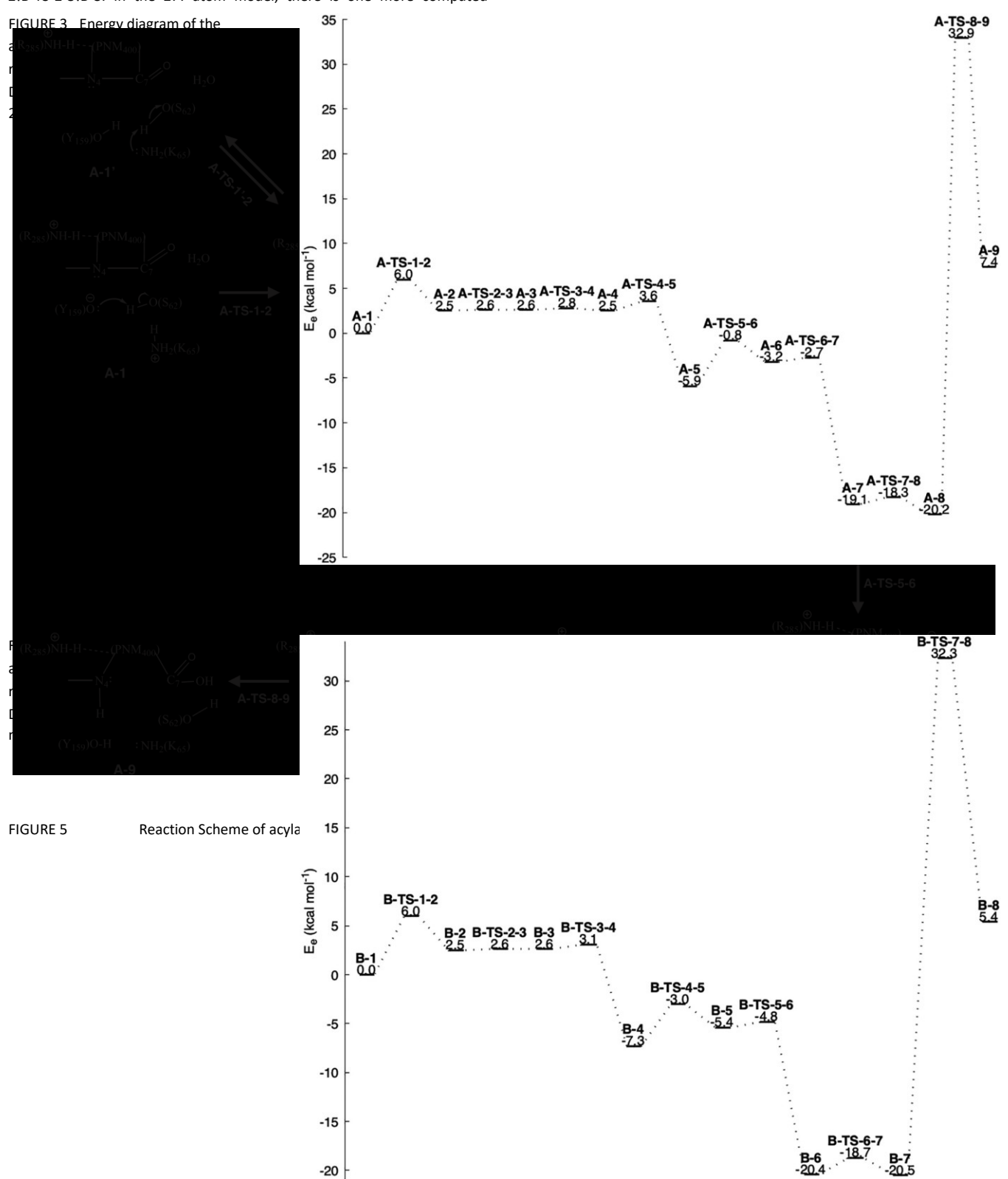
## 3.1 | Acylation reaction

In the 277-atom model, stepping from the acylation reactant K+Y^-(A1) to the intermediate (A-2), the proton on Ser62-Oy transfers to Tyr159-O in Scheme 1, where Tyr159 in the anionic form reacts as the general base. In this step, the Lys65 stays protonated throughout. This step leads to a basic intermediate A-2 which is slightly higher in energy than A-1 ( $\Delta\Delta E = 2.5$  kcal mol<sup>-1</sup>) with an activation energy of 6.0 kcal mol<sup>-1</sup>. The distance between Ser62-Oy and PNM400-C<sub>7</sub> changes from 2.63 Å in A-1 to 2.54 Å in A-2. This elementary step also starts off the acylation in the 278-atom model path, with the same activation energy of 6.0 kcal mol<sup>-1</sup>. The distance between Ser62-Oy and PNM400-C<sub>7</sub> similarly changes from 2.58 in B-1 to 2.49 Å in B-2. The proton transfer is followed by a translation of the

6-membered ring on the ligand, where the ring moves away from Phe120 with a 2.6 kcal mol<sup>-1</sup> energy of activation in the 277-atom model. The effective energy of activation for the elementary step A2!A-TS-2-3!A-3 is only 0.1 kcal mol<sup>-1</sup>. The similar transition state has also been found in the 278-atom model with a same 2.6 kcal mol<sup>-1</sup> energy of activation, and an effective energy of activation of 0.1 kcal mol<sup>-1</sup> for the elementary step B-2!B-TS-2-3!B-3. In the 277-atom model, there is one more computed

intermediate before Ser62-O $\gamma$  bonds to PNM400-C $_7$ , in which small geometric shifts of PNM Wat1108 and Wat1330 occur. The effective activation energy of A-3!A-TS-3-4!A-4 is 0.2 kcal mol $^{-1}$ ).

Next, nucleophilic addition takes place with an effective activation energy of 1.1 kcal mol<sup>-1</sup> in the 277-atom model, where Ser62-O $\gamma$  covalently bonds to C $\gamma$  of the substrate (Scheme 2,  $r(O\gamma-C_7)$  = 1.49 Å in A-5). The hydroxyl group in Tyr159 rotates so that the hydrogen forms a stronger



hydrogen bond with N<sub>4</sub> of the substrate. In this step, r(H N<sub>4</sub>) changes from 2.90 to 1.72 Å from A-4 to A-5. The activation 277-atom model

energy for this step is 3.6 kcal mol<sup>-1</sup>, and A-4 is 2.5 kcal mol<sup>-1</sup> higher while A-

The proton transfer from Lys65 to Tyr159 is observed in both the 277atom (A-TS-7-8) and 278-atom models (B-TS-6-7), forming the K<sup>0</sup>Y<sup>0</sup> protonation state (A-8 and B-7) with effective activation energies of 0.8 and 1.7 kcal mol<sup>-1</sup>. No deacylation transition states could be isolated with a K<sup>+</sup>Y<sup>-</sup> protonation state of the acyl-enzyme complex, in both the 277- and 278-

FIGURE 6 Reaction Scheme of acylation and deacylation of penicillin G reaction with Streptomyces R61 DD-peptidase in solution via the 5 is 5.9 kcal mol<sup>-1</sup> lower in energy than A-1, respectively. After the acylenzyme complex is formed, the water molecules close to Ser62 reorient and move closer to the substrate in preparation for the ring opening of the substrate. A-6 is also a tetrahedral intermediate and is 3.2 kcal mol<sup>-1</sup> lower in energy than A-1.

In the 278-atom model, the activation energy is 3.1 kcal mol<sup>-1</sup> for formation of the tetrahedral intermediate and it leads to a low energy product B-4, which is 7.3 kcal mol<sup>-1</sup> lower in energy than B-1. Similar to the 277-atom model, after the acyl-enzyme complex is formed, the waters close to Ser62 reorient and move closer to the substrate, resulting in the B-5 tetrahedral intermediate that is 5.4 kcal mol<sup>-1</sup> lower in energy than B-1.

In the next step (Scheme 3) the proton from the Tyr159 hydroxyl group transfers to N<sub>4</sub> causing the four-membered ring on the substrate to open in both the 277-atom and 278-atom models. The length of r(H N<sub>4</sub>) further shortens to 1.02 Å in A-7 (1.02 Å in B-6), and the Tyr159 side chain becomes basic. This elementary step is barrierless in both the 277-atom and 278atom models, and it leads to the very stable acyl-enzyme covalent bond complex, A-7 that is 19.1 kcal mol<sup>-1</sup> lower in energy than A-1, or B-6 which

20.4 kcal mol<sup>-1</sup> lower than B-1.

atom models. Based on the energetics of this study, the acylation reaction would likely be irreversible, as the k-2 rate would be extremely slow and endergonic.

#### Comparison of acyl-enzyme 3.2 intermediates with X-ray crystal structure

The starting input geometry for both models was based on the X-ray crystal structure of the penicilloyl acyl enzyme complex, (PDB: 1PWC). Closely resembling the crystal structure, the acylation product 278-atom model

A-8 in the 277-atom model was found to be the most stable intermediate. and it is 20.2 kcal mol<sup>-1</sup> lower in energy in the proposed mechanism compared to A-1. The corresponding structure in the 278-atom model is B-7, which is the K<sup>0</sup>Y<sup>0</sup> form of the acyl-enzyme complex and is lower in energy than the B-6 intermediate (K+Y-, corresponding to A-7).

Effectively barrierless transition states lead to the lowest energy acylintermediates (A-8 and B-7), which are shown in Figures 3 and 4 to be thermodynamic sinks along the energy diagram, which matches previous descriptions of the " $\beta$ -lactam trap character" of R61 DD-peptidase. <sup>[20]</sup> In Figure 7, A-8 (in magenta) and B-7 (in orange) are overlaid on top of the corresponding fragment from the 1PWC X-ray crystal structure (in green). The carbonyl oxygen (O<sub>8</sub>) in the substrate PNM400 is stabilized by Thr301 and is also hydrogen bonded to Asn161 in both A-8 and B-7. Previous studies have found that Thr301 is important for acylation <sup>[49]</sup> and Asn161 is important for deacylation. <sup>[17]</sup> The O<sub>13</sub> of the carboxylate on PNM400 in both models hydrogen bonds with Thr299, which is found to be important in acylation. <sup>[49]</sup> As there are no geometric restraints on the substrate, the phenyl ring in PNM400 shifts in both the 277- and 278-atom models, promoting the geometric shift of the Phe120 and Trp233 side chains to form  $\pi$ - $\pi$  interactions (named the "hydrophobic patch" by others<sup>[14]</sup>).

In the acyl-enzyme structure, a proton on His298-N $_{\delta}$  can form a hydrogen bond with the Thr299 main chain oxygen (1.66 Å), which does not contribute to the catalytic mechanism, and this hydrogen bond is observed in computed intermediates of the 278-atom model. The His298-N $_{\epsilon}$  proton forms a hydrogen bond with Tyr159-O, and a slightly longer O-H bond distance is observed in the 277-atom model (2.17 Å) compared to the 278-atom model (2.10 Å). Thus, the acylenzyme complex in both models holds

the hydroxyl oxygen in position for proton transfer from/to Ser62-Oy. The activation energy in the acylation portion of the proposed mechanism relative to the initial enzyme-substrate non-covalently bound complex is 3.6 kcal mol<sup>-1</sup> in the 277-atom model and 3.1 kcal mol<sup>-1</sup> in the 278-atom model leading to the formation of the tetrahedral intermediate. These computed activation energies throughout the acylation pathway are much lower than that derived from experimental kinetics.<sup>[52]</sup>

## 3.3 | Protonation state of His298

The proposed acylation mechanism (and deacylation mechanism described below) for the 277-atom and 278-atom models are thermodynamically, kinetically, and structurally similar. To further probe the most likely His298 protonation state, the  $pK_a$  value of the His298-N $_{\delta}$  proton was calculated using a thermodynamic cycle. [86] Gas phase geometry optimization and frequency computations of the A-8 and B-7 acyl-intermediates were computed. Using values of -265.9 kcal  $mol^{-1}$  for the solvation energy of a proton, [86] our computed  $pK_a$  value for the

SCHEME 1 Proton transfer from Ser

$$\begin{array}{c} \bigoplus \\ (R_{285}) NH-H--(PNM_{400}) \\ & \stackrel{\bullet}{N_4} - C_7 \\ & \stackrel{\bullet}{N_2} O \\ & \stackrel{\bullet}{(Y_{159})O}: H \\ & \stackrel{\bullet}{O}(S_{62}) \\ & \stackrel{\bullet}{H_2} O \\ & \stackrel{\bullet}{N_4} - C_7 \\ & \stackrel{\bullet}{N$$

$$\begin{array}{c} \bigoplus \\ (R_{285})NH-H--(PNM_{400}) \\ \hline \\ N_4 \\ \hline \\ (Y_{159})O \end{array} \\ \begin{array}{c} \bigoplus \\ H_2O \end{array} \\ \begin{array}{c} \bigoplus \\ (R_{285})NH-H--(PNM_{400}) \\ \hline \\ (R$$

Phe120
PNM400
Phe120
Trp233
Tyr159
Asn161
Thr299 Ser62

His298
Lys65

FIGURE 7 Overlay of the optimized 278-atom structure B-7 (in orange without hydrogen atoms) 277-atom structure A-8 (in magenta without hydrogen atoms) with the trimmed fragment from X-ray crystal structure of 1PWC (in green)

His298-N $_{\delta}$  proton is 11.1, which is substantially greater than that of the N $_{\delta}$  proton in free aqueous histidine (~6.0). The strongly basic His298 also does not have any nearby His, Glu, or Asp residues that could easily accept the N $_{\delta}$  proton. Though an in vivo ensemble average of His298 protonation states likely exists, computational evidence suggests this residue is doubly-protonated. This provides atomic-level agreement with the findings of Hargis, Woodcock, and co-authors, who applied QM/MM orbital analyses with variation of relevant amino acid residue protonation states to determine that doubly protonated His298 had the most favorable active site interactions. [31]

## 3.4 | Deacylation reaction

With the formation of A-8 in the 277-atom model ( $K^0Y^0$ , B-7 in the 288-atom model), the Lys65-N becomes a proton acceptor so that a nearby water molecule (Wat1014 in the 1PWC X-ray crystal structure) can donate a proton to Lys65, while the water oxygen can bond to  $C_7$  on the substrate (Scheme 5). The 277- and 278-atom models for the deacylation transition states are very similar structurally. A-TS8-9 and B-TS-7-8 have a  $C_7$ -O<sub>wat</sub> bond distance of 1.93/1.93 Å, a  $C_7$ -O $_{7-Ser}$  bond distance of 1.57/1.57 Å, and a  $C_7$ -O $_{8}$  bond distance of 1.21/1.22 Å, respectively.

In a previous computational study of deacylation in the acyl-CBL complex, a tetrahedral intermediate has been described. [87] Tyr159 could act as a general base to abstract a proton from a second water molecule in the CBL active site, while a proton transfers from Lys to Ser. [57-59] However, in our study, there is no such second water in our models (derived from the 1PWC X-ray crystal structure) close to Tyr159. In our models, the Ser62 residue is the only base. The OH group of the single available water binds with C<sub>7</sub> on the substrate; water dissociation and proton transfer are concerted in our computations. Similar acid/base chemistry is predicted in the 278-atom model B-TS-7-8). The effective activation energies in the 277atom model (ATS-8-9) and 278-atom model (B-TS-7-8) are 53.1 and 52.8 kcal  $\text{mol}^{-1}$ , respectively. The  $\Delta E_{\text{rxn}}$  of A-8 to A-9 and B-7 to B-8 are predicted to be 32.9 and 32.3 kcal mol<sup>-1</sup>, respectively. Thus, the deacylation (hydrolysis) reaction is the rate-limiting step, in agreement with previous experiment and expectations for substrate inhibition kinetics/thermodynamics. [18,19] The computed effective energies of activation for the deacylation transition state are in agreement with a previous computational study that shows values of 49.2 and 40.0 kcal mol<sup>-1</sup>.[57] This insurmountable barrier would not be significantly lowered even with a second nearby water in the active site.

#### 3.5 Kinetics and thermodynamics of the inhibition pathway

For antibiotics to be effective, they must competitively and irreversibly bind to the DD-peptidase active site, preventing enzyme binding to natural substrates. The proposed kinetics of antibiotic inhibition of DD-peptidase has been given as:

$$E + C_k $^{+1}_{1} E C_k $^{+2}_{2} E - C_k !^{+3}_{1} E + P$$

where E is the enzyme, C is the  $\beta$ -lactam antibiotic inhibitor or natural substrate, E C is the non-covalent Henri-Michaelis complex, and E - C\* is the acyl-enzyme complex.[16,17,48,49,52,88-91] k+1, k+2, and k+3 are first-order

ruled out. Our computations (and previous work) confirm that peptidoglycan substrates and larger penicillins provide a very tight fit in the active site.

Computationally designed antibiotics for DD-peptidase require facile enzyme-substrate binding (larger  $k_{+2}$ /smaller  $\Delta G^{\ddagger}$ ) and effectively negligible rates for deacylation ( $k_{+3}$  approaching zero/larger  $\Delta G^{\ddagger}$ ). For comparison, natural substrates tripeptide (Ac2-L-Lys-D-Ala-D-Ala) and thioester substrate hippuryl thioglycollate (C<sub>6</sub>H<sub>5</sub>\_CO NH \_CH<sub>2</sub>CO S CH<sub>2</sub>\_COO<sup>-</sup>) have been found to react with the wildtype enzyme Streptomyces R61 DD-peptidase at rates of  $k_{+2}$  = 55 and 6 s<sup>-1</sup>, respectively (which correspond to activation free energies of ~15.2 and ~16.5 kcal mol<sup>-1</sup>) at 37C. [52] In that same work, the rate constants k+2 and k+3 of the Streptomyces R61 DD-peptidase reacting with the inhibitor penicillin G (in Figure 8) were determined to be 180 and  $1.4 \times 10^{-4} \, \text{s}^{-1}$  at 37C, respectively. [52] Thus, when penicillin G concentration was present, a 40,000-fold decrease in the rate constant of product formation occurred, (which corresponds to an activation free energy of ~22.9 kcal mol-1).

It is important to note that Frère and co-authors[15] refer to the formation of the acyl-enzyme complex with  $\beta$ -lactams as the terminal product (with a measured pseudo-first order rate constant of inactivation), rather than the deacylation products. This implies a rate constant of zero for subsequent deacylation once an acyl-enzyme complex of the inhibitor is formed. However, concentration of both the natural peptidoglycan substrate and  $\beta$ -lactam inhibitor is present in the experimental inhibition study. Frère and coauthors also write the "deacylation rate was determined by measuring the recovery of enzyme activity after complete inactivation and addition of  $\beta$ -lactamase to rapidly eliminate the excess of free antibiotic." We suspect that the experimentally measured pseudo-first order rate constant of inactivation  $(k_{+3})$  is actually the product rate constant of k-2 \*k-1, which correlates with the reverse acylation and subsequent dissociation of the inhibitor. In vivo, such a manipulation of  $\beta$ -lactamase concentration would not possible to drive equilibrium back towards the E + C complex. Our computed reverse activation energy of acylation k-2; [ΔE(B-

FIGURE 8 The acylation and deacylation reaction mechanism for penicillin G and serine protease type enzyme rate constants of the formation of the E C, E - C\*, and E + P. Competitive inhibition, where both inhibitor and natural substrate co-exist in the enzyme active site, was originally suggested by Frère, [18,88] but then later

7)  $-\Delta E(B-TS-1-2)$ ] = 26.5 kcal mol<sup>-1</sup> suggests very slow kinetics at physiological temperature. Rather than acting as a competitive inhibitor,

penicillin G functions as a mechanistic-based inactivator, or suicide inhibitor.

Though  $k_2$  is accelerated ( $\Delta G^{\ddagger}$  = 14.5 kcal mol<sup>-1</sup>) when penicillin G was added to the reaction by Josephine et al,<sup>[15]</sup> our computations show a much smaller activation energy for the acylation process ( $\Delta E^{\ddagger}$  = 6.0 kcal mol<sup>-1</sup>). However, this aspect of the kinetics may be a more troublesome comparison between theory and experiment due to substrate posing and diffusion processes. The kinetics and thermodynamics presented in Figures 3 and 4 do show excellent agreement with a QM/MM study of acylation of class A  $\beta$ -lactamase,<sup>[92]</sup> which found the acylation transition state is 4.5 kcal mol<sup>-1</sup> higher in energy than the Michaelis complex, and the tetrahedral acylintermediate is

5.4 kcal mol<sup>-1</sup> lower in energy than the E C complex.

#### 4 | CONCLUSIONS

The inhibitor penicillin G reacts with the Streptomyces R61 DDpeptidase through a general base catalytic path. From large 277and 278-atom QM cluster models, the proposed mechanism of acylation and deacylation has been modeled with Density Functional Theory. Either Lys65 (K<sup>0</sup>Y<sup>0</sup>) or Tyr159 (K+Y-) can act as the general base, but basic Tyr159 is more energetically favorable, which is in agreement with other studies. [23,24,51] However, we find in our QM enzyme models that only the K+Y- protonation state can productively lead to the acylation transition state. The general base abstracts a proton from Ser62-Oy leading to Ser62-Oy nucleophilic attack of C<sub>7</sub> on the substrate, forming a very stable acyl-enzyme complex. The acylation transition state activation energies in our study are predicted to be  $\Delta E^{\ddagger}$  = 3.6 kcal mol<sup>-1</sup> in the 277-atom model and 3.1 kcal mol<sup>-1</sup> in the 278atom model, which are lower than the experimentally reported value for the natural peptidoglycan substrate.<sup>[52]</sup> Similar to the findings in a previous high level QM/MM study, [92] the computed acylation activation barrier is significantly lower than experimental prediction. Overall, penicillin G acts as a suicide inhibitor in DD-peptidase. In this situation, which is validated by our theoretical exploration of the coupling of acylation and deacylation processes, (a) the acylation of the inhibitor is kinetically fast, (b) the acylenzyme complex falls into a thermodynamic sink, and deacylation is kinetically impossible, and (c) reactivation of the enzyme via reverse acylation of the inhibitor is kinetically slow (but not infinitely so).

The acyl-enzyme complex of both the 277 and 278-atom models resembles the structure of the X-ray crystal structure. At the atomic-level, our DFT results crucially validate penicillin G as a ligand that can strongly bind to Streptomyces R61 DD-peptidase. The reverse acylation reaction has an activation energy of 26.2 kcal mol<sup>-1</sup> from A-8 to A-TS-1-2 of the 277-atom model, and 26.5 kcal mol<sup>-1</sup> from B-7 to B-TS-1-2 of the 278-atom model, which may correspond to the experimentally determined enzyme recovery activation energy of about 23 kcal mol<sup>-1</sup>.

The acyl-enzyme complex must first undergo proton transfer from  $K^+Y^-$  to  $K^0Y^0$  to promote deacylation. Even though  $K^+Y^-$  and  $K^0Y^0$  protonation states

are nearly isoenergetic, the latter form favors proton transfer from water to Ser62 to facilitate the deacylation. However, identifying the appropriate acyl-enzyme protonation states may be biochemically insignificant, given the irreversibility of acylation, and the insurmountable activation energy of deacylation. Once the antibiotic is covalently bound to the enzyme and "resides" in the proposed thermodynamic sink, it serves its purpose to inhibit the cell wall cross-linking ability of DD-peptidase. The in vivo deacylation mechanism of DD-peptidase with peptidoglycan may require a different protonation state for the Lys65-Tyr159 pair and could be influenced by nearby water molecules in the active site, but the reported QM-cluster model computations show complete inhibition of deacylation. Application of the QM-cluster model to study different antibiotics and contrast proposed mechanisms with native peptidoglycans is a promising future avenue of investigation.

The proposed mechanism details structures located along the enzyme reaction path that are in good agreement with experimental observation and other theoretical studies. Similar to other studies on QM cluster models performed in our laboratory,  $^{[68,69]}$  building models via the Residue Interaction Network increases the rigor and reproducibility when studying enzymatic reaction mechanisms, as it can help to identify the key residues involved in the reaction, and automatically provides the atomic-level models. Our automated approach to QMcluster modeling, via the RINRUS software toolkit being developed in our group, provides efficient and high-quality models that provide chemical insight into the detailed acylation/deacylation processes of antibiotics that target DD-peptidase. Overall, the current study replicates the gross behavior of  $\beta$ -lactam inhibition, provides answers to lingering novel questions about the atomic-level mechanism of DDpeptidase, and demonstrates the robustness of reproducible QMcluster models generated by RINRUS.

## **ACKNOWLEDGMENTS**

The authors would like to thank Professors Daniel L. Baker (University of Memphis) and H. Lee Woodcock (University of South Florida) for insightful discussions. This work was supported by the National Science Foundation (CAREER Grant BIO-1846408) and start-up funding from the University of Memphis Department of Chemistry. This work was also supported in part by a grant from The University of Memphis College of Arts and Sciences Faculty Research Grant Fund. This support does not necessarily imply endorsement by the University of research conclusions. The High Performance Computing Center and the Computational Research on Materials Institute at The University of Memphis (CROMIUM) also provided generous resources for this research.

Additional Supporting Information may be found in the online version of this article.

- A Results of proton transfer pathway from Ser to Lys for acylation.
- B Thermochemical data of all reported minima/maxima of the penicil-lin G reaction with Streptomyces R61 DD-peptidase.
- C Cartesian coordinates of the optimized stationary points along the 277atom model and 278-atom model pathways. All xyz-formatted files are

contained in the archive. Charge of the 277-atom model (structures with "A" prefix) is neutral. Charge of the 278-atom model (structures with "B" prefix) is +1.

#### ORCID

Qianyi Cheng https://orcid.org/0000-0002-4640-2238

Nathan J. DeYonker https://orcid.org/0000-0003-0435-2006

#### **ENDNOTE**

1 RINRUS takes the X-ray crystal structure file, utilizes the Residue Interaction Network information, extracts important residues, and automatically constructs/trims/builds models for QM and QM/MM calculations. The RINRUS toolkit will be open-source and shared with the computational chemistry/biology communities in parallel with a forthcoming introductory/tutorial publication. We encourage interested readers to contact the authors for more information.

#### **REFERENCES**

- [1] B. G. Spratt, Microbiology 1983, 129, 1247. https://doi.org/10.1099/ 00221287-129-5-1247.
- [2] A. Pechenov, M. E. Stefanova, R. A. Nicholas, S. Peddi,
  - W. G. Gutheil, Biochemistry 2003, 42, 579. https://doi.org/10.1021/bi026726k.
- [3] A. P. Kuzin, H. Liu, J. A. Kelly, J. R. Knox, Biochemistry 1995, 34, 9532. https://doi.org/10.1021/bi00029a030.
- [4] R. A. Powers, E. Caselli, P. J. Focia, F. Prati, B. K. Shoichet, Biochemistry 2001, 40, 9207. https://doi.org/10.1021/bi0109358.
- [5] J. M. Frère, B. Joris, G. D. Shockman, CRC Crit. Rev. Microbiol. 1984, 11, 299. https://doi.org/10.3109/10408418409105906.
- [6] A. L. Demain, R. P. Elander, Antonie Van Leeuwenhoek 1999, 75, 5. https://doi.org/10.1023/A:1001738823146.
- [7] D. J. Tipper, J. L. Strominger, Proc. Natl. Acad. Sci. U. S. A. 1965, 54, 1133. https://doi.org/10.1073/pnas.54.4.1133.
- [8] D. J. Tipper, Pharmacol. Ther. 1985, 27, 1. https://doi.org/10.1016/0163-7258(85)90062-2.
- [9] J.-M. Frère, B. Joris, L. Varetto, M. Crine, Biochem. Pharmacol. 1988, 37, 125. https://doi.org/10.1016/0006-2952(88)90764-2.
- [10] V. H. A. Hirvonen, K. Hammond, E. I. Chudyk, M. A. L. Limb, J. Spencer, A. J. Mulholland, M. W. van der Kamp, J. Chem. Inf. Model. 2019, 59, 3365. https://doi.org/10.1021/acs.jcim.9b00442.
- [11] C. L. Tooke, P. Hinchliffe, E. C. Bragginton, C. K. Colenso, V. H. A. Hirvonen, Y. Takebayashi, J. Spencer, J. Mol. Biol. 2019, 431, 3472. https://doi.org/10.1016/j.jmb.2019.04.002.
- [12] A. Maxwell, C. G. Dowson, J. Spencer, J. Mol. Biol. 2019, 431, 3367. https://doi.org/10.1016/j.jmb.2019.06.018.
- [13] Development & Approval Process (Drugs), https://www.fda.gov/drugs/developmentapprovalprocess/default.htm, (accessed September 17, 2018).
- [14] N. R. Silvaggi, H. R. Josephine, A. P. Kuzin, R. Nagarajan, R. F. F. Pratt, J. A. Kelly, J. Mol. Biol. 2005, 345, 521. https://doi.org/10.1016/j.jmb.2004.10.076.
- [15] H. R. Josephine, I. Kumar, R. F. Pratt, J. Am. Chem. Soc. 2004, 126, 8122. https://doi.org/10.1021/ja048850s.
- [16] M. Jamin, J. M. Wilkin, J. M. Frère, Biochemistry 1993, 32, 7278. https://doi.org/10.1021/bi00079a026.
- [17] J. M. Wilkin, M. Jamin, B. Joris, J. M. Frère, Biochem. J. 1993, 293, 195. https://doi.org/10.1042/bj2930195.
- [18] A. Marquet, J. M. Frère, J. M. Ghuysen, A. Loffet, Biochem. J. 1979, 177, 909. https://doi.org/10.1042/bj1770909.

- [19] J. M. Ghuysen, Annu. Rev. Microbiol. 1991, 45, 37. https://doi.org/10. 1146/annurev.mi.45.100191.000345.
- [20] R. F. Pratt, J. Chem. Soc. Perkin Trans. 2002, 2, 851. https://doi.org/ 10.1039/b107097p.
- [21] D. J. Waxman, J. L. Strominger, Annu. Rev. Biochem. 1983, 52, 825. https://doi.org/10.1146/annurev.bi.52.070183.004141.
- [22] A. Dubus, S. Normark, M. Kania, M. G. P. Page, Biochemistry 1994, 33, 8577. https://doi.org/10.1021/bi00194a024.
- [23] M. I. Page, B. Vilanova, N. J. Layland, J. Am. Chem. Soc. 1995, 117, 12092. https://doi.org/10.1021/ja00154a009.
- [24] A. Dubus, P. Ledent, J. Lamotte-Brasseur, J.-M. Frère, Proteins Struct. Funct. Genet. 1996, 25, 473. https://doi.org/10.1002/(SICI)10970134(199608)25:4<473::AID-PROT7>3.0.CO;2-E.
- [25] J. Lamotte-Brasseur, A. Dubus, R. C. Wade, Proteins Struct. Funct. Genet. 2000, 40, 23. https://doi.org/10.1002/(SICI)1097-0134 (20000701)40:1<23::AID-PROT40>3.0.CO;2-7.
- [26] B. M. Beadle, I. Trehan, P. J. Focia, B. K. Shoichet, Structure 2002, 10, 413. https://doi.org/10.1016/S0969-2126(02)00725-6.
- [27] Y. Kato-Toma, T. Iwashita, K. Masuda, Y. Oyama, M. Ishiguro, Biochem. J. 2003, 371, 175. https://doi.org/10.1042/bj20021447.
- [28] Y. Chen, A. McReynolds, B. K. Shoichet, Protein Sci. 2009, 18, 662. https://doi.org/10.1002/pro.60.
- [29] R. Tripathi, N. N. Nair, J. Phys. Chem. B 2012, 116, 4741. https://doi. org/10.1021/jp212186q.
- [30] R. Tripathi, N. N. Nair, J. Am. Chem. Soc. 2013, 135, 14679. https://doi.org/10.1021/ja405319n.
- [31] J. C. Hargis, J. K. White, Y. Chen, H. L. Woodcock, J. Chem. Inf. Model. 2014, 54, 1412. https://doi.org/10.1021/ci5000517.
- [32] Y.-M. Ahn, R. F. Pratt, Bioorg. Med. Chem. 2004, 12, 1537. https://doi.org/10.1016/j.bmc.2003.12.042.
- [33] J. C. Hargis, S. L. Vankayala, J. K. White, H. L. Woodcock, J. Chem. Theory Comput. 2014, 10, 855. https://doi.org/10.1021/ct400968v.
- [34] S. A. Adediran, S. A. Deraniyagala, Y. Xu, R. F. Pratt, Biochemistry 1996, 35, 3604. https://doi.org/10.1021/bi952107i.
- [35] L. Maveyraud, R. F. Pratt, J.-P. Samama, Biochemistry 1998, 37, 2622. https://doi.org/10.1021/bi972501b.
- [36] A. Matagne, J. Lamotte-Brasseur, J.-M. Frère, Biochem. J. 1998, 330, 581. https://doi.org/10.1042/bj3300581.
- [37] N. Díaz, D. Suárez, T. L. Sordo, K. M. Merz, J. Phys. Chem. B 2001, 105, 11302. https://doi.org/10.1021/jp012881h.
- [38] N. Díaz, T. L. Sordo, K. M. Merz, D. Suárez, J. Am. Chem. Soc. 2003, 125, 672. https://doi.org/10.1021/ja027704o.
- [39] Y. Fujii, N. Okimoto, M. Hata, T. Narumi, K. Yasuoka, R. Susukita,
  A. Suenaga, N. Futatsugi, T. Koishi, H. Furusawa, A. Kawai, T. Ebisuzaki,
  S. Neya, T. Hoshino, J. Phys. Chem. B 2003, 107, 10274. https://doi.org/10.1021/jp034536t.
- [40] J. C. Hermann, L. Ridder, A. J. Mulholland, H.-D. Höltje, J. Am. Chem. Soc. 2003, 125, 9590. https://doi.org/10.1021/ja034434g.
- [41] J. C. Hermann, C. Hensen, L. Ridder, A. J. Mulholland, H.-D. Höltje, J. Am. Chem. Soc. 2005, 127, 4454. https://doi.org/10.1021/ja044210d.
- [42] R. Li, J.-M. Liao, C.-R. Gu, Y.-T. Wang, C.-L. Chen, J. Phys. Chem. B 2011, 115, 10298. https://doi.org/10.1021/jp111572v.
- [43] C. Oefner, A. D'Arcy, J. J. Daly, K. Gubernator, R. L. Charnas, I. Heinze, C. Hubschwerlen, F. K. Winkler, Nature 1990, 343, 284. https://doi.org/10.1038/343284a0.
- [44] C. Fenollar-Ferrer, J. Frau, B. Vilanova, J. Donoso, F. Muñoz, J. Mol. Struct. Theochem. 2002, 578, 19. https://doi.org/10.1016/S01661280(01)00675-3.
- [45] R. F. Pratt, Cell. Mol. Life Sci. 2008, 65, 2138. https://doi.org/10.

- 1007/s00018-008-7591-7.
- [46] K. TSUKAMOTO, K. TACHIBANA, N. YAMAZAKI, Y. ISHII, K. UJHE, N. NISHIDA, T. SAWAI, Eur. J. Biochem. 1990, 188, 15. https://doi. org/10.1111/j.1432-1033.1990.tb15365.x.
- [47] K. Tsukamoto, N. Nishida, M. Tsuruoka, T. Sawai, FEBS Lett. 1990, 271, 243. https://doi.org/10.1016/0014-5793(90)80416-G.
- [48] J. M. Wilkin, M. Jamin, C. Damblon, G. H. Zhao, B. Joris, C. Duez, J. M. Frère, Biochem. J. 1993, 291, 537. https://doi.org/10.1042/bj2910537.
- [49] J. M. Wilkin, A. Dubus, B. Joris, J. M. Frère, Biochem. J. 1994, 301, 477. https://doi.org/10.1042/bj3010477.
- [50] D. Monnaie, A. Dubus, J. M. Frère, Biochem. J. 1994, 302, 1. https://doi.org/10.1042/bj3020001.
- [51] E. Lobkovsky, E. M. Billings, P. C. Moews, J. Rahil, R. F. Pratt, J. R. Knox, Biochemistry 1994, 33, 6762. https://doi.org/10.1021/bi00188a004.
- [52] A. M. Hadonou, M. Jamin, M. Adam, B. Joris, J. Dusart,
  - J. M. Ghuysen, J. M. Frère, Biochem. J. 1992, 282, 495. https://doi.org/10.1042/bj2820495.
- [53] J.-M. Wilkin, J. Lamotte-Brasseur, J.-M. Frère, Cell. Mol. Life Sci. 1998, 54, 726. https://doi.org/10.1007/s000180050200.
- [54] B. P. Atanasov, D. Mustafi, M. W. Makinen, Proc. Natl. Acad. Sci. U. S. A. 2000, 97, 3160. https://doi.org/10.1073/pnas.97.7.3160.
- [55] D. B. Boyd, Proc. Natl. Acad. Sci. U. S. A. 1977, 74, 5239. https://doi. org/10.1073/pnas.74.12.5239.
- [56] N. Díaz, D. Suárez, T. L. Sordo, Biochemistry 2006, 45, 439. https://doi.org/10.1021/bi051600j.
- [57] B. F. Gherman, S. D. Goldberg, V. W. Cornish, R. A. Friesner, J. Am. Chem. Soc. 2004, 126, 7652. https://doi.org/10.1021/ja036879a.
- [58] M. Hata, Y. Tanaka, Y. Fujii, S. Neya, T. Hoshino, J. Phys. Chem. B 2005, 109, 16153. https://doi.org/10.1021/jp045403q.
- [59] R. Tripathi, N. N. Nair, J. Phys. Chem. B 2016, 120, 2681. https://doi. org/10.1021/acs.jpcb.5b11623.
- [60] M. J. J. M. Zvelebil, M. J. E. Sternberg, Protein Eng. Des. Sel. 1988, 2, 127. https://doi.org/10.1093/protein/2.2.127.
- [61] P. Csermely, Trends Biochem. Sci. 2008, 33, 569. https://doi.org/10. 1016/i.tibs.2008.09.006.
- [62] S. Vishveshwara, A. Ghosh, P. Hansia, Curr. Protein Pept. Sci. 2009, 10, 146. https://doi.org/10.2174/138920309787847590.
- [63] M. Vendruscolo, E. Paci, C. M. Dobson, M. Karplus, Nature 2001, 409, 641. https://doi.org/10.1038/35054591.
- [64] A. Giuliani, A. Krishnan, J. Zbilut, M. Tomita, Curr. Protein Pept. Sci. 2008, 9, 28. https://doi.org/10.2174/138920308783565705.
- [65] L. Swint-Kruse, Biochemistry 2004, 43, 10886. https://doi.org/10. 1021/bi049450k.
- [66] L. Swint-Kruse, C. S. Brown, Bioinformatics 2005, 21, 3327. https://doi.org/10.1093/bioinformatics/bti511.
- [67] N. J. DeYonker, C. E. Webster, J. Am. Chem. Soc. 2013, 135, 13764. https://doi.org/10.1021/ja4042753.
- [68] N. J. DeYonker, C. E. Webster, Biochemistry 2015, 54, 4236. https://doi.org/10.1021/acs.biochem.5b00396.
- [69] T. J. Summers, Q. Cheng, N. J. DeYonker, N. J. DeYonker, Org. Biomol. Chem. 2018, 16, 4090. https://doi.org/10.1039/C8OB00540K.
- [70] J. M. Word, S. C. Lovell, J. S. Richardson, D. C. Richardson, J. Mol. Biol. 1999, 285, 1735. https://doi.org/10.1006/jmbi.1998.2401.
- [71] J. M. Word, S. C. Lovell, T. H. LaBean, H. C. Taylor, M. E. Zalis, B. K. Presley, J. S. Richardson, D. C. Richardson, J. Mol. Biol. 1999, 285, 1711. https://doi.org/10.1006/jmbi.1998.2400.
- [72] M. J. Frisch, G. W. Trucks, H. B. Schlegel, G. E. Scuseria, M. A. Robb,
   J. R. Cheeseman, G. Scalmani, V. Barone, G. A. Petersson,
   H. Nakatsuji, X. Li, M. Caricato, A. V Marenich, J. Bloino,

- B. G. Janesko, R. Gomperts, B. Mennucci, H. P. Hratchian, J. V Ortiz,
- A. F. Izmaylov, J. L. Sonnenberg,
  - D. Williams-Young, F. Ding,
- F. Lipparini, F. Egidi, J. Goings, B. Peng, A. Petrone, T. Henderson,
- D. Ranasinghe, V. G. Zakrzewski, J. Gao, N. Rega, G. Zheng, W. Liang,
- M. Hada, M. Ehara, K. Toyota, R. Fukuda, J. Hasegawa, M. Ishida,
- T. Nakajima, Y. Honda, O. Kitao, H. Nakai, T. Vreven, K. Throssell,
- J. A. Montgomery Jr., J. E. Peralta, F. Ogliaro, M. J. Bearpark, J. J. Heyd, E. N. Brothers, K. N. Kudin, V. N. Staroverov, T. A. Keith,
- R. Kobayashi, J. Normand, K. Raghavachari, A. P. Rendell, J. C. Burant, S. S. Iyengar, J. Tomasi, M. Cossi, J. M. Millam, M. Klene, C.
- Adamo, R. Cammi, J. W. Ochterski, R. L. Martin, K. Morokuma, O. Farkas, J. B. Foresman, D. J. Fox, Gaussian 16 Revision B.01.
- Gaussian Inc., Wallingford, CT 2016.
- [73] C. Lee, W. Yang, R. G. Parr, Phys. Rev. B 1988, 37, 785. https://doi. org/10.1103/PhysRevB.37.785.
- [74] A. D. Becke, J. Chem. Phys. 1993, 98, 5648. https://doi.org/10.1063/ 1.464913
- [75] P. C. Hariharan, J. A. Pople, Theor. Chim. Acta 1973, 28, 213. https://doi.org/10.1007/BF00533485.
- [76] G. A. Petersson, M. A. Al-Laham, J. Chem. Phys. 1991, 94, 6081. https://doi.org/10.1063/1.460447.
- [77] J. B. Foresman, Æ. Frisch Eds., Exploring chemistry with electronic structure methods, 2nd ed., Gaussian Inc, Pittsburgh, PA 1996, p. 278.
- [78] W. J. Hehre, R. Ditchfield, J. A. Pople, J. Chem. Phys. 1972, 56, 2257. https://doi.org/10.1063/1.1677527.
- [79] S. Grimme, S. Ehrlich, L. Goerigk, J. Comput. Chem. 2011, 32, 1456. https://doi.org/10.1002/jcc.21759.
- [80] S. Grimme, J. Antony, S. Ehrlich, H. Krieg, J. Chem. Phys. 2010, 132, 154104. https://doi.org/10.1063/1.3382344.
- [81] V. Barone, M. Cossi, J. Phys. Chem. A 1998, 102, 1995. https://doi. org/10.1021/jp9716997.
- [82] M. Cossi, N. Rega, G. Scalmani, V. Barone, J. Comput. Chem. 2003, 24, 669. https://doi.org/10.1002/jcc.10189.
- [83] P. E. M. Siegbahn, M. R. A. Blomberg, Chem. Rev. 2000, 100, 421. https://doi.org/10.1021/cr980390w.
- [84] M. R. A. Blomberg, T. Borowski, F. Himo. R.-Z. Liao.
  - P. E. M. Siegbahn, Chem. Rev. 2014, 114, 3601. https://doi.org/10. 1021/cr400388t.
- [85] R. G. Letterman, C. B. Duke, T. T. To, T. J. Burkey, C. E. Webster, Organometallics 2014, 33, 5928. https://doi.org/10.1021/om5007165.
- [86] J. Ho, Phys. Chem. Chem. Phys. 2015, 17, 2859. https://doi.org/10. 1039/C4CP04538F.
- [87] N. J. Bernstein, R. F. Pratt, Biochemistry 1999, 38, 10499. https://doi. org/10.1021/bi990428e.
- [88] J.-M. Frère, J.-M. Ghuysen, H. R. Perkins, Eur. J. Biochem. 1975, 57, 353. https://doi.org/10.1111/j.1432-1033.1975.tb02308.x.
- [89] J.-M. Frère, C. Duez, J.-M. Ghuysen, FEBS Lett. 1976, 70, 257. https://doi.org/10.1016/0014-5793(76)80770-3.
- [90] M. I. Page, Acc. Chem. Res. 1984, 17, 144. https://doi.org/10.1021/ar00100a005.
- [91] H. Christensen, M. T. Martin, S. G. Waley, Biochem. J. 1990, 268, 808. https://doi.org/10.1042/bj2680808a.
- [92] J. C. Hermann, J. Pradon, J. N. Harvey, A. J. Mulholland, J. Phys. Chem.
   A. 2009, 113, 11984. https://doi.org/10.1021/jp9037254.



## SUPPORTING INFORMATION

Additional supporting information may be found online in the Supporting Information section at the end of this article.

How to cite this article: Cheng Q, DeYonker NJ. Acylation and deacylation mechanism and kinetics of penicillin G reaction with Streptomyces R61 DD-peptidase. J Comput Chem. 2020;

41:1685-1697. https://doi.org/10.1002/jcc.26210